A DETACHED EDDY SIMULATION STUDY OF THE HORSESHOE VORTEX SYSTEM IN THE FLOW PAST A BRIDGE ABUTMENT WITH A SCOUR HOLE AT A HIGH REYNOLDS NUMBER

Mete KOKEN[1] and George CONSTANTINESCU[2]

[1]Research Assistant, Dept. of Civil and Env. Eng., University of Iowa
(IIHR Hydroscience & Engineering, Iowa City, IA 52242-1585, USA)
E-mail:mkoken@uiowa.edu
[2]Assistant Professor, Dept. of Civil and Env. Eng., University of Iowa
(IIHR Hydroscience & Engineering, Iowa City, IA 52242-1585, USA)
E-mail:sconstan@engineering.uiowa.edu

A numerical investigation using Detached Eddy Simulation (DES) is conducted to study the dynamics of the horseshoe vortex system forming at the base of a bridge abutment and the associated turbulence amplification related with the bi-modal oscillations of the primary necklace vortex. The abutment has the shape of a vertical wall and is situated in a straight open channel with a scoured bed corresponding to equilibrium conditions at the end of the scour process. The bathymetry is obtained from experiment. In both experiment and simulation, the channel Reynolds number is 250,000 and the incoming flow is fully turbulent. The turbulence amplification associated with the presence of the bi-modal oscillations peaks in vertical sections parallel to the streamwise direction situated in between the lateral wall and the tip of the abutment. In these sections a double-peak distribution is observed for the turbulent kinetic energy and the pressure r.m.s. fluctuations. In the mean flow, an elongated coherent structure is present above the main necklace vortex. Though less energetic, this eddy interacts and exchanges vorticity with the main necklace vortex. The largest values of the pressure r.m.s. fluctuations at the bed are observed along the upstream face of the abutment and are induced by the strong temporal variations in the intensity of the downflow.

Key Words : *local scour, bridge abutments, numerical simulations, coherent strucutres*

1. INTRODUCTION

Bridge abutments are hydraulic structures build out from the river bank. The presence of a bridge abutment in an alluvial channel causes a very complex three dimensional (3D) highly turbulent flow field (Fig. 1) to occur within its proximity as a result of the separation of the incoming boundary layer, formation of the detached shear layer (DSL) at the tip of the abutment, and the wake flow past it. In rivers, where there is continuous change of the bathymetry due to erosion, the nonlinear interactions between the mobile bed and the local flow around the abutment further complicate the problem. Large bed shear stresses and pressure fluctuations can be induced in some bed regions around the base of the structure. As a result, scour will develop around it. This scouring may be excessive and cause the weakening of the bridge foundation. Consequently, stability problems may arise which can eventually lead to bridge failure. Therefore, understanding the flow physics associated with the scouring process and predicting the scour evolution and maximum scour depth around bridge abutments has been one of the most important research topics in river engineering (e.g., see Melville, 1997).

As the flow approaches the abutment, as a result of the adverse pressure gradients, the incoming boundary layer separates and necklace like vortical structures form around the base of the structure. These vortices form what is known as the horseshoe vortex (HV) system. The necklace vortices follow the

junction line between the bed and the upstream face of the structure. Then, they bend in the direction of the flow as it passes the abutment. These necklace vortices are thought to control, to a great extent, the evolution of the scour process at the base of the upstream face of the abutment. The turbulent HV system around surface-mounted bluff bodies is very unsteady and subject to large temporal variations of its location, size and intensity. Furthermore, it was observed the turbulent kinetic energy (TKE) and pressure r.m.s. fluctuations are significantly amplified within the HV system (Devenport and Simpson, 1990; Kirkil et al., 2008) and large bed shear stress and pressure fluctuations are induced on the bed region beneath the HV system. This explains the determinant role played by the HV system in the development of the scour hole.

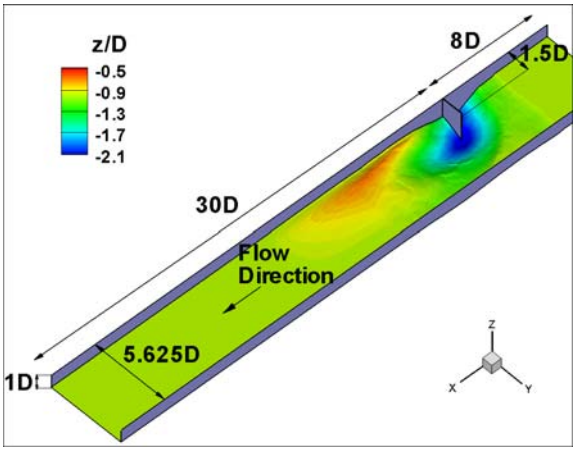

Fig.1 Computational domain with bathymetry contours corresponding to equilibrium scour conditions

The present investigation focuses on the characterization of the structure of the HV system in the instantaneous and mean flow fields at conditions close to equilibrium scour for an abutment placed in a straight channel with vertical lateral walls. The channel Reynolds number is Re=240,000 and a vertical wall perpendicular to the lateral walls plays the role of an abutment of simplified geometry. The equilibrium bathymetry is obtained from an experiment conducted at the same Reynolds number. Due to the large value of the Reynolds number, the present numerical simulation employs a non-zonal hybrid Reynolds-Averaged Navier Stokes (RANS) - Large Eddy Simulation (LES) method called Detached Eddy Simulation (e.g., see Constantinescu and Squires, 2004). Eddy-resolving numerical simulations provide 3D visualizations of the entire (averaged and instantaneous) flow field. This allows an easier study of the dynamics of the main coherent structures in the flow and the nature of their interactions with other coherent structures or with the bed. This investigation is similar to the one (Koken and Constantinescu, 2007) conducted in our group using LES at a lower channel Reynolds number (Re=18,000). Scale effects are due not only to the difference in the Reynolds number but also to the different shape of the scour hole in the two simulations.

2. NUMERICAL MODEL & SIMULATION SETUP

A general description of the DES code is given in Constantinescu and Squires (2004). The 3D incompressible Navier-Stokes equations are integrated using a fully-implicit fractional-step method. The governing equations are transformed to generalized curvilinear coordinates on a non-staggered grid. Convective terms in the momentum equations are discretized using a blend of fifth-order accurate upwind biased scheme and second-order central scheme. All other terms in the momentum and pressure-Poisson equations are approximated using second-order central differences. The discrete momentum (predictor step) and turbulence model equations are integrated in pseudo-time using alternate direction implicit (ADI) approximate factorization scheme. In the present DES simulation, the Spalart-Allmaras (SA) one-equation model was used. Time integration in the DES code is done using a double time-stepping algorithm and local time stepping is used to accelerate the convergence at each physical time step. The time discretization is second order accurate.

The length scale is selected to be the flow depth (D). The mean velocity in the main channel (U) is used as the velocity scale. The abutment length is 1.5D and is located at a distance of 8D from the inflow section (see Fig. 1). The physical time is 0.02D/U. The computational domain is meshed using 7.5 million cells in DES. A minimum grid spacing of one wall unit was used in the wall normal direction.

At the inflow section, turbulent inflow conditions corresponding to fully developed turbulent channel flow are applied. The velocity fields from a preliminary periodic channel LES simulation at Re=18,000 are stored in a file and then fed in a time-accurate manner through the inflow section in the simulations containing the abutment. The mean streamwise velocity profile at Re=240,000 is obtained from a preliminary RANS simulation and the turbulent fluctuations at Re=18,000 are superimposed on the mean profile. At the outflow, a convective boundary condition is used. The free surface is treated as a rigid lid which is justified as the

channel Froude number is 0.2 in experiment. The walls are treated as no-slip boundaries. The bathymetry is obtained from an experiment (D=0.53m, U=0.45m/s) conducted under clearwater scour conditions. The sediment size of the loose bed is d_{50}=1.05 mm. The maximum flow depth is 2.34D.

3. RESULTS

The Q criterion is used in Fig. 2 to visualize the coherent structures in the upstream recirculation region and inside the scour hole. A coherent structure whose axis is initially vertical is present. Then its axis bends as the bottom of the scour hole is approached. This structure corresponds to the main corner vortex (CV1) in the upstream recirculation region. Its role is to convect fluid and momentum from the free surface into the core of the main necklace vortex HV1, similar to the low Reynolds number deformed-bed case discussed in Koken and Constantinescu (2007). However, there is a significant difference between these two cases. Another eddy, denoted HV2, is present starting close to the lateral wall. It also draws fluid from the free surface. HV2 is situated inside the scour hole but at higher levels than HV1. Near the lateral wall, HV2 is situated farther away from the abutment. As the abutment is approached, HV2 becomes closer to the extremity of the abutment. This means the axes of HV1 and HV2 are not parallel. In this sense, HV2 does not play the usual role of a secondary necklace vortex. Such necklace vortices are, in fact, present inside the scoured region, a short distance from the separation line of the incoming boundary layer (coherent structures HV3 and HV4 in Fig. 2). The presence of HV2 is not so much a direct consequence of the difference in the Reynolds number with the simulation discussed in Koken and Constantinescu (2007). Rather, it is a result of the different bathymetry shape in the scour hole region and larger relative scour depth. Analysis of the instantaneous flow fields show that ejections of patches of opposite sign vorticity to the one inside HV1 are observed regularly in the near bed region. HV4 is, in fact, a counter-rotating bottom-attached vortex induced by the presence of HV1 in the near-bed region.

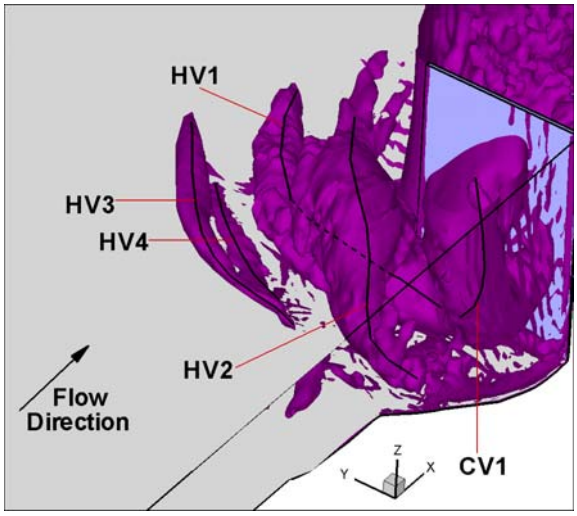

Fig.2 Visualization of vortical structure of the mean flow around the abutment using the Q criterion.

The TKE and pressure r.m.s. fluctuations (Fig. 3) are strongly amplified above the levels corresponding to the surrounding turbulent flow in the region where the core of HV1 is oscillating. However, non-dimensional values are about 50% lower in the present simulations compared to the ones in the low Reynolds number case. Most probably this is due to the fact that the core of HV1 is more stable in the present higher Reynolds number simulation. The larger depth of the scour hole may also limit the amplitude of the large-scale aperiodic oscillation of the core of HV1 that are the primary factor responsible for the high turbulence levels. This appears to be the case especially in the sections situated around the tip of the abutment and downstream of it (sections b and c in Fig. 3) where the region of high TKE amplification is relatively circular and the TKE peaks at the center of the region. By contrast, the region of high TKE values in section a, that is parallel to the wall and intersects the abutment at around 0.5D from its tip, has a more elliptical shape which has two peaks. This suggest that in the high Reynolds number case the intensity of the large-scale oscillations of the core of HV1 peaks in sections situated between the lateral wall of the channel and the tip of the abutment. In the low Reynolds number deformed-bed simulation the levels of TKE amplification were the highest at sections cutting through the tip of the abutment.

The position of the region of very large pressure r.m.s. fluctuations is not always similar in the low and the high Reynolds number simulations. At sections situated between the lateral wall and the tip of the abutment the distributions are qualitatively very similar. However, at sections cutting through the tip of the abutment and through the leg of HV1 (sections b and c in Fig. 3) the pressure r.m.s.

fluctuations are strongly amplified inside a small patch situated close to the bed. This patch is part of the larger region of relatively amplification of the pressure r.m.s. fluctuations and TKE induced by the large-scale oscillations of HV1. Also, this patch is distinct from the small patch of high r.m.s. pressure fluctuations corresponding to the corner vortex present at the junction line between the bed and the abutment. The high pressure r.m.s. fluctuations inside these two patches adjacent to the bed have obvious consequences for sediment entrainment from the deeper parts of the scour hole. By contrast, in the low Reynolds number case (see Koken and Constantinescu, 2007), the region of high pressure r.m.s. fluctuations inside the scour bed was situated at a significantly larger distance from the bed.

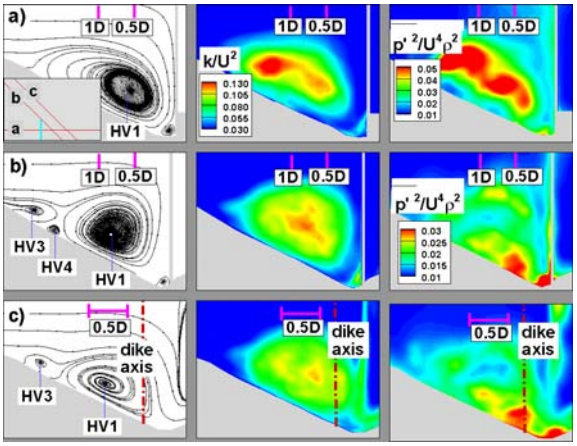

Fig. 3 Streamlines, resolved TKE and pressure r.m.s. fluctuations in representative vertical sections (see inset in frame a)

Similar to the low Reynolds number deformed-bed case discussed in Koken and Constantinescu (2007), the structure of the primary necklace vortex HV1 undergoes significant changes in time and its core is subject to large-scale oscillations. These oscillations are the main reason of the strong amplification of the TKE and pressure fluctuations inside the scour hole.

At sections situated in between the lateral wall and the tip of the abutment (e.g., see the corresponding 2D streamline patterns and velocity vectors in the section shown in Fig. 4) the structure of the flow inside the scour hole is similar to that observed in the low Reynolds number simulation both when the vortex is in the zero-flow mode (core of HV1 is more compact and fairly circular) and in the back-flow mode (core of HV1 is larger and has a more elliptical shape). The axis of HV1 moves by close to 0.5D as the core of HV1 oscillates between these two preferred states. This explains the two-peak distribution of the TKE at the same section (Fig. 4c). Observe also the presence of a relatively strong eddy upstream of HV1 in the zero-flow mode. This eddy may be associated with HV2 in the mean flow.

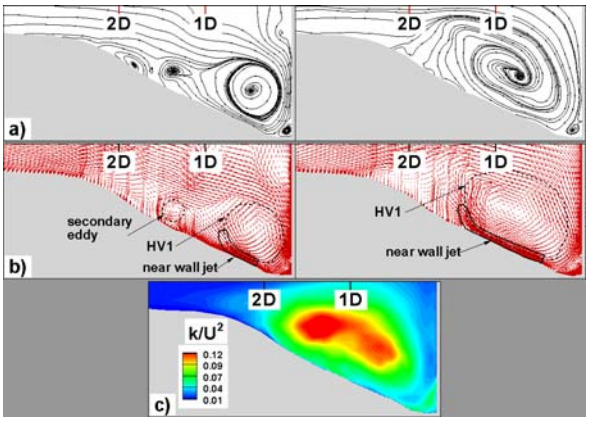

Fig. 4 Instantaneous flow 2D streamline patterns (a) and velocity vectors (b) in a plane parallel to the lateral wall (see inset) corresponding to the zero-flow mode (left frames) and the back-flow mode (right frames) oscillations of the primary necklace vortex HV1. Also shown is the TKE distribution (c) in the same section

The main difference with the low Reynolds number case is that the intensity of the bi-modal oscillations does not peak anymore in the sections cutting through the tip of the abutment, but rather in the sections situated in between the lateral wall and the tip of the abutment. One suspects this is less a direct effect of the increase of the Reynolds number, but rather an indirect effect due to the different shape and larger relative depth of the scour hole in the present high Reynolds number simulation.

The distribution of the pressure r.m.s. fluctuations at the bed is given in Fig. 5. This quantity is very important as it determines together with the value of the bed shear stress whether or not sediment particles will be entrained from the bed. Accurate estimation of $\overline{p'^2}$ from experimental measurements is practically impossible. Eddy resolving simulations allow estimating this important quantity characterizing the intensity of the turbulence in the near bed region. The largest values of $\overline{p'^2}$ are observed along the upstream face of the abutment and are induced by the strong temporal variations in the intensity of the downflow parallel to the upstream face of the abutment. Similar levels of amplification are observed beneath the upstream part of the DSL and on the face of the submerged hill (see Fig. 1) over which the DSL eddies are convected in the near-bed region. Finally, $\overline{p'^2}$ is also strongly amplified over the opposite side of the submerged hill.

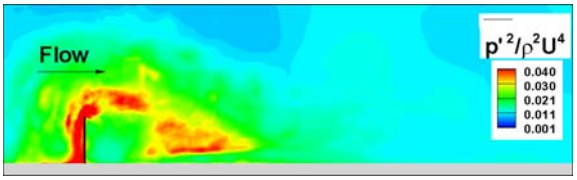

Fig. 5 Non-dimensional pressure r.m.s. fluctuations at the bed

4. SUMMARY

DES was used to investigate the flow past an abutment of simplified geometry (vertical wall) on a deformed bed corresponding to equilibrium scour conditions. The channel Reynolds number was 240,000. The attached boundary layers were sufficiently well resolved in the wall-normal direction to avoid the use of wall functions. The incoming flow was fully turbulent and contained turbulent fluctuations.

Similar to the low Reynolds number deformed-bed simulation at Re=18,000 discussed in Koken and Constantinescu (2007), the core of main necklace vortex of the HV system was found to undergo large-scale bi-modal oscillations. The main corner vortex in the upstream recirculation region feeds fluid and momentum from the free surface region into the core of the main necklace vortex. However, the turbulence amplification associated with the presence of the large-scale oscillations was found to peak in vertical sections parallel to the streamwise direction situated in between the lateral wall and the tip of the abutment. In these sections, a double-peak distribution was observed for the TKE and pressure r.m.s. fluctuations. This is different from the low-Reynolds-number deformed-bed case where the intensity of the large-scale oscillations peaked in vertical sections cutting through the tip of the abutment. Another difference with the low Reynolds number case was the presence, in the mean flow, of a coherent structure situated above the main necklace vortex. Though less energetic, this structure was found to interact and exchange vorticity with the main necklace vortex. One suspects both these differences are mostly due to the different shape of the scour hole in the low and high Reynolds number simulations. Finally, DES allowed determination of the distribution of the pressure r.m.s. fluctuations at the bed that together with the bed shear stress determine whether or not sediment particles will be entrained from the bed. The largest amplification of the pressure r.m.s. fluctuations was in the region where the eddies convected with the downflow reach the bed.

REFERENCES

1) Constantinescu, G. and Squires, K.: Numerical investigations of flow over a sphere in the subcritical and supercritical regimes, *Phys. of Fluids*, Vol. 16, No. 5, pp. 1449-1466, 2004.
2) Devenport, W. J. and Simpson, R. L.: Time-dependent and time-averaged turbulence structure near the nose of a wing-body junction, *J. Fluid Mechanics*, Vol. 210, pp. 23-55, 1990.
3) Kirkil, G., Constantinescu, S.G. and Ettema, R.: Coherent structures in the flow over a circular bridge pier at equilibrium scour conditions, in press, ASCE J. of Hydr. Engrg., 2008.
4) Koken, M. and Constantinescu, S.G.: An investigation of coherent structures in the wake of a bridge abutment at equilibrium bed scour conditions, 2007 World Water and Environmental Resources Congress, Tampa, Florida, May 2007.
5) Melville, B. W.: Pier and abutment scour: integrated approach, J. Hydr. Engrg., Vol. 123, No. 2, pp. 125-136, 1997.